JOURNAL OF MATERIALS SCIENCE **36** (2001) 3963–3971

On the mechanosorptive effect in porous ceramics

Part I *Experimental results*

J. LEPAGE
Laboratoire de Science et Génie des Surfaces, LSGS, UMR 7570 CNRS, Ecole des Mines, Parc de Saurupt, 54042 Nancy Cédex, France
E-mail: lepage@mines.u-nancy.fr

The interaction of water with porous media is still a controversial topic. Hydration of most materials softens them but numerous exceptions exist. The visco-elastic properties are also affected and two experimental facts are of interest. Firstly, the damping factor increases with the coverage up to a monolayer. Secondly, it presents a maximum beyond this coverage. During drying, this huge peak has been interpreted as a mechanosorptive effect, i.e. stress assisted adsorption. During adsorption, the stress state of H-bonded solids changes, leading to enhanced viscoelastic dissipation. This first paper provides experimental evidences of the H-bonding in solids, a detailed discussion of the mechanisms operative in mechanosorption is postponed to a forthcoming one.

1. Introduction

In a series of publications [1–3] we analysed the mechanical behaviour of various porous media when soaked in water. As regard to Young's or storage modulus E, porous media can be divided into two classes. In the first one, E is a still growing function of the water content. In the second one, E is a monotonous decreasing function of the same parameter. The loss tangent or damping factor Q^{-1} is generally a growing function of the water content, however during drying experiments, unexpected maxima can be resolved [3].

This paper presents new results on alumina and chalk, two materials that present the above mentioned maximum [3]. Former works on porous silica glass (Vycor) [1, 2] and graphite are also of interest to the problem and will be revisited here. On alumina, two types of samples have been considered, hydroxide-free and gibbsite-containing alumina. A large part of this paper is devoted to establish a clear distinction among these samples, especially as a function of the annealing temperature T_a.

2. Experimental section

2.1. Experimental technique

Dynamical Mechanical Spectroscopy (DMS) at room temperature has been described in previous publications [2, 3]. It allows us to measure the Young's modulus E and the damping factor Q^{-1} of parallelepiped samples the length of which is 100 mm long and the cross section 5×10 mm^2, as a function of time or as a function of the water content. The water content is measured by Sw, ratio of the actual content of water in the sample to its water content after prolonged soaking in liquid water. The water content at saturation is 6×10^{-2} g of water per gram of dry solid for alumina, 15×10^{-2} g/g for chalk and 0.28 g/g for Vycor. Taking into account the porosity of the samples, these values indicate that the pores are fully wetted by water and that only open porosity exists.

A typical experiment is as follows. After a one hour heat treatment in air at temperature T_a, the sample is allowed to adsorb water vapour from the laboratory air ($t = 22°C$, HR = 55%) while the parameters of interest E, Q^{-1} and Sw are periodically recorded. After the apparent saturation of the adsorption from the gas phase, the sample is soaked in distilled water for 300s. The same parameters are then recorded during drying. Fig. 1 represents the schematic evolution of the parameters versus time.

2.2. Materials studied

The main physical properties of the materials are presented in Table I. New results have been obtained only on alumina and chalk. Vycor glass and graphite are described here because the results soon obtained on these materials are of interest to the discussion. In the last column of Table I, labelled ratio of YM, the numerator refers to the Young's modulus (in GPa) of the material under study while the denominator refers to the Young's modulus of the same material at full density. 70 GPa is the Young's modulus of fused silica. Chalk is assumed to be all calcite. E is calculated from C_{12} and C_{44} for calcite (84 GPa) and alumina (370 GPa) [4]. This ratio gives an indication on the deleterous effect of porosity on the mechanical properties of the material [5].

TABLE I

	chemical composition	mean porosity%	mean pore diameter	BET surface area As (m^2/g)	maximum water content (g/g)	ratio of YM
Vycor	SiO_2	28	4 nm	200	0.25	17/70
Chalk	$CaCO_3$	15	200nm	2	0.15	12/84
alumina	Al_2O_3	25	25μm	0.2	0.06	90/370
Graphite	pure carbon	depends on oxidation 30 → 50		depends on oxidation 45 → 12	depends on oxidation 0 → 0.10	12/80

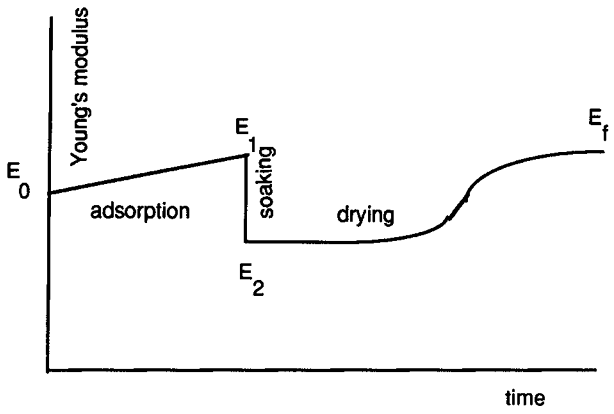

Figure 1 Schematic variations of the Young's modulus during a typical experiment.

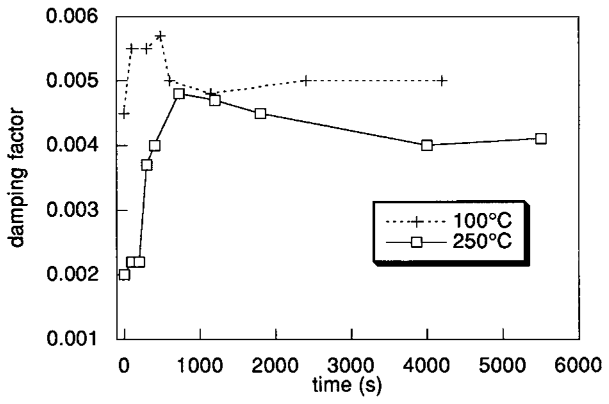

Figure 3 Damping factor of chalk against time of adsorption at two temperatures of annealing T_a. On the 250°C curve the time to the maximum corresponds to the completion of the bound water layer. This time lag is absent on the 100°C curve since the bound water layer exists at the start of the experiment.

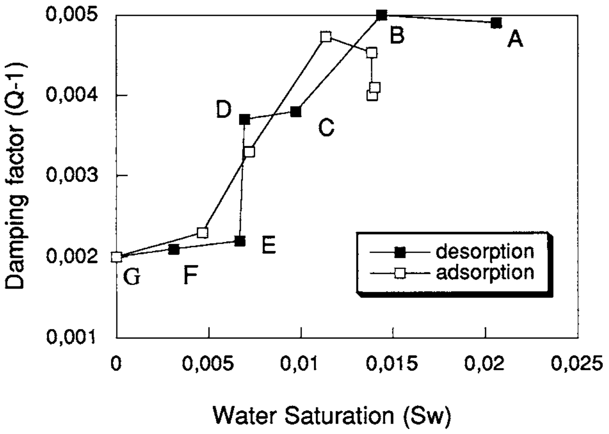

Figure 2 Damping factor of chalk versus the total (bound + free) water saturation Sw of the sample. Filled symbols refer to an experiment after isothermal desorption at the indicated temperature. (A) $T_a = 25°C$, (B) $T_a = 50°C$, (C) $T_a = 75°C$, (D) $T_a = 100°C$, (E) $T_a = 125°C$, (F) $T_a = 175°C$, (G) $T_a = 250°C$.

2.2.1. Chalk

2.2.1.1. Adsorption from the laboratory air. Chalk samples equilibrated at 50% RH contains 3.5×10^{-3} g/g ($Sw = 2.3 \times 10^{-2}$) of water desorbable by heating at 250°C. On Fig. 2, filled symbols, the damping factor is measured as soon as possible after an isothermal desorption at the indicated temperature of a previously air-equilibrated sample. The origin of the abscissa axis is deduced from the weight of a sample after outgassing at 250°C which is considered in an arbitrary fashion as the upper limit of desorption of bound water. The adsorption curve (open symbols) is obtained at 20°C while water vapour is adsorbing at the surface after a 250°C outgassing. Two regions are apparent on these curves. The low coverage one where the damping factor increases linearly with the water content and the high water content where the damping factor saturates and even slightly decreases. This behaviour is more clearly pictured on Fig. 3 where Q^{-1} is plotted as a function of time. The open square symbols, labelled 250°C, are the results already presented on Fig. 2 where the outgassing temperature before experiment is 250°C. To obtain the curve labelled 100°C, the outgassing temperature before experiment is reduced to 100°C in order to desorb only free water without affecting the bound water layer. In a somewhat arbitrary fashion, water physisorbed on solids is classified as free water if its desorption temperature is below 105°C [6] and as bound water if the desorption temperature lies in the 105°C–250°C interval. Beyond 250°C the mass losses result from the condensation of hydroxyls, i.e. water chemisorbed dissociatively, and their evaporation. During adsorption, water adsorbs first in the bound state at a high rate, then in the free state at a much reduced rate. On oxides, especially silica, adsorption in the bound state is associated with the presence of hydroxyls to which water molecules bind by hydrogen bonding [7–10]. Free water adsorbs on top of the bound layer at high relative humidity (RH > 50%). If the surface is devoid from hydroxyls, water adsorbs in the free state on metal or oxygen sites by dispersion forces at a much reduced rate. On calcite the situation is not so well documented but it is expected that the distinction between bound and free water, based on the rate

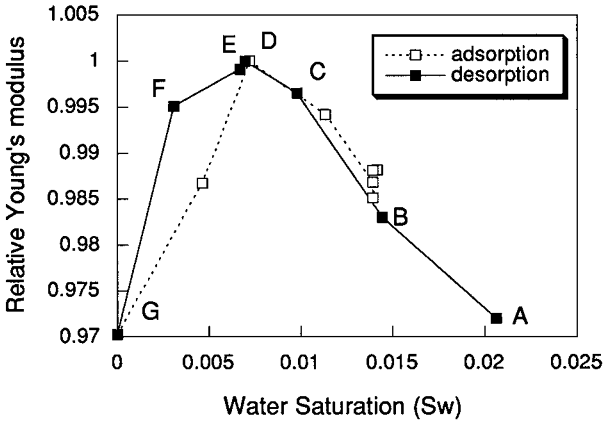

Figure 4 Young's modulus of chalk against the total (bound + free) water saturation Sw. The filled symbols are obtained similarly to the corresponding points in Fig. 2. The curve labelled "adsorption" is obtained after annealing at *G* and is an indication of the reversibility of the process under study.

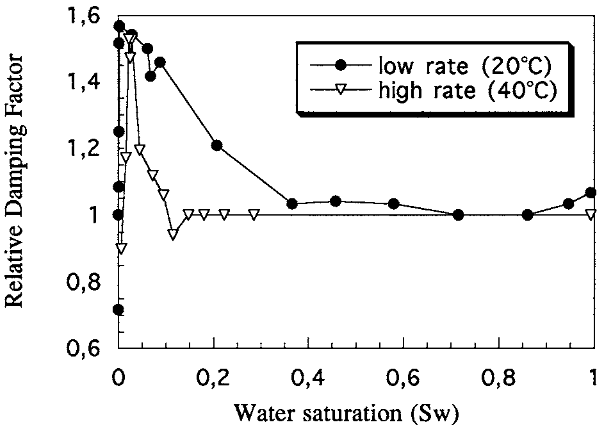

Figure 5 Damping factor of chalk during drying out of a previously soaked sample at two drying temperatures 20°C and 40°C.

of adsorption and the temperature of desorption is still valid. From the results presented in Fig. 2 and Fig. 3 it is clear that bound water enhances the mechanical damping of the solids while free water acts in an opposite way.

The same behaviour can be noticed in the evolution of the Young's modulus depicted on Fig. 4 which is the analog of Fig. 2 (during an experiment E and Q^{-1} are obtained simultaneously). The filled symbols, labelled from A to G, refer to the desorption experiment previously described on Fig. 2. At 50% RH on calcite, thermogravimetry reveals that 2×10^{-3} g/g are adsorbed in the free state while 1×10^{-3} g/g are adsorbed in the bound state. Taking into account the BET surface area A_s reported in Table I, the reported water contents correspond to 1 monolayer and 0.5 monolayer respectively. From these results it is clear that minute amounts of bound water enhance E and Q^{-1} while free water lowers them. In the literature the enhancement of Q^{-1} during water adsorption on minerals is well documented [11–15] but the distinction between free and bound water is not emphasised. Furthermore the maximum in Q^{-1}, though apparent on the drawings, is not discussed.

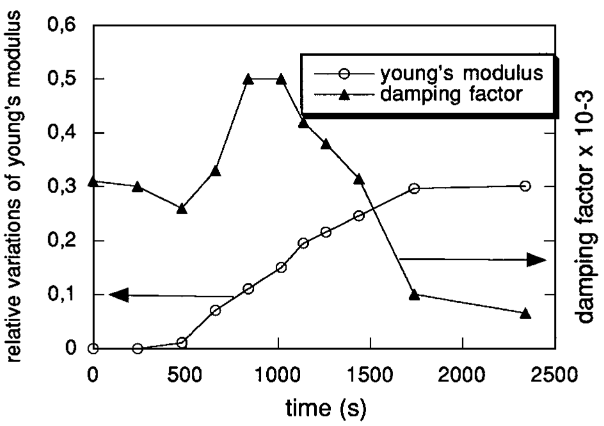

Figure 6 Damping factor (right hand side) and relative variation of the Young's modulus (left hand side) of chalk during drying at 20°C. The maximum of the damping factor takes place during the steepest variations of the Young's modulus.

2.2.1.2. Drying of a previously soaked sample. The rate of drying $\frac{dm}{dt}$ can be varied by gently heating the sample during measurement. On Fig. 5 the damping factor Q^{-1} has been plotted as a function of the water content measured by Sw at two drying temperatures 20°C and 40°C. As frequently quoted, during the desorption of the so-called capillary state, i.e. bulk free water, no changes in the mechanical properties of the sample intervene [11, 12, 14]. At intermediate water content (Sw = 0.06) a huge peak in Q^{-1} can be resolved. In the very dry state, as usual, the damping factor is very low. The width of the peak under study is considerably reduced at high heating rates, i.e. at high temperature and one may wonder whether it would still exist at higher temperature. On Fig. 6 the Young's modulus has been plotted as a function of time beside the above described damping factor. Clearly the maximum in the $Q^{-1}_{(Sw)}$ curve can be associated with the steepest slope in the $E_{(Sw)}$ curve as in classical viscoelasticity. A complete discussion of this result is postponed to a following paper.

2.2.2. Alumina

As mentioned early, alumina samples used in this study present a large variability as regard to their initial hydroxyl content. The thermogramm of a highly hydroxylated sample presented in Fig. 7 bears large similarities with that of gibbsite though this phase cannot be identified by X Ray Diffraction (XRD) on our samples. The net mass loss of the alumina sample presented in Fig. 7 is very large, 2×10^{-2}, but is generally 6×10^{-3} on most samples, which corresponds, on a mass basis, to a gibbsite concentration of 2×10^{-2}. The total mass loss of pure gibbsite on heating at 700°C is 33.9%, in good agreement with the theoretical value of 34.6% corresponding to the decomposition reaction

$$2Al(OH)_3 \longrightarrow Al_2O_3 + 3H_2O. \qquad (1)$$

A gibbsite concentration lower than 2×10^{-2} is not detectable by XRD since the spectra of alpha alumina and of gibbsite are very similar. Moreover, other

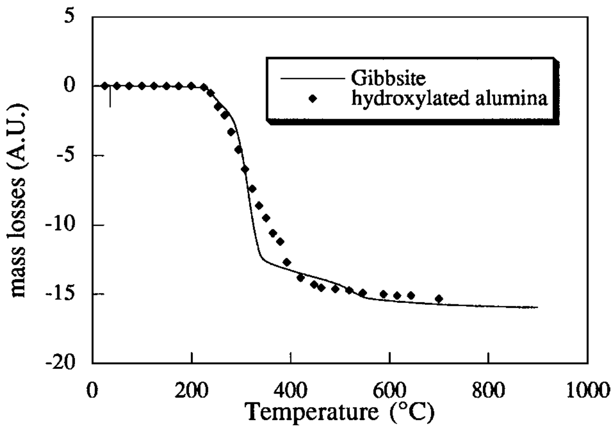

Figure 7 Thermogramms of a hydroxyl containing alumina sample and of pure gibbsite. Total mass loss of the alumina sample, 6×10^{-3} g/g. Total mass loss of the pure gibbsite sample 0.34 g/g.

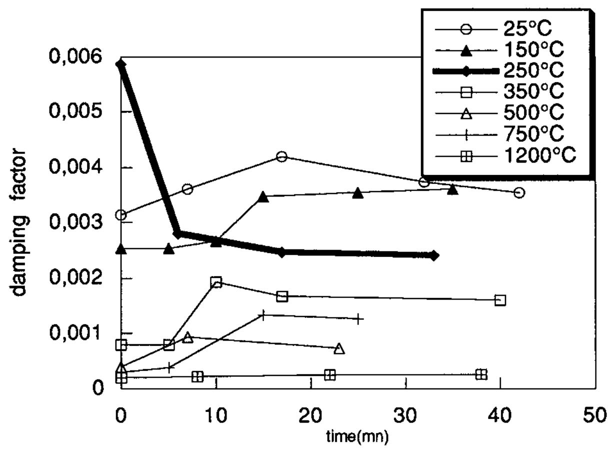

Figure 8 Damping factor of a gibbsite containing alumina sample during adsorption from the laboratory air after annealing at various temperatures.

hydrated phase such as boehmite may be present in the sample. Whatever is the intimate nature of the hydroxylated phase, it is considered as a source of hydrogenated species to the inner surfaces of the pores.

2.2.2.1. Damping factor variations during water vapour adsorption from the laboratory air. The experimental procedure has been described in Section 2.1. In Fig. 8, Q^{-1} is plotted as a function of the adsorption time elapsed after an one hour annealing at the indicated temperature. At the exception of the 250°C curve that deserves further comments, the behaviour of alumina is reminiscent of chalk. Samples annealed at $T_a < 250$°C have a high initial damping factor, the relative variations of which during adsorption are rather small. Annealing the sample at $T_a < 350$°C lowers the initial (water-free) damping factor while the subsequent relative variation is rather large. At the exception of the 1200°C curve which is flat throughout the time domain investigated, a shallow maximum can be resolved on most curves. Fig. 9 illustrates the dependence of the initial (water-free) damping factor on the temperature of annealing T_a for hydroxyl containing (mass loss on 1200°C heating 6×10^{-3}g/g) and hydroxyl-free samples (mass loss on 1200°C heating $< 10^{-4}$g/g). On the hydroxylated sample the peak at $T_a = 250$°C is superposed on a slowly decreasing background. The two curves are identical at $T_a > 500$°C where the gibbsite decomposition is complete. On Fig. 10 are presented the Young's modulus variations during adsorption for some selected temperatures of annealing which are collected simultaneously with those presented on Fig. 8. The loss of the initial Young's modulus is streaking in the 200°C–400°C range and is associated with the gibbsite decomposition that occurs at that temperature. Water vapour adsorption increases slightly E at the exception of the 250°C curve where the gain in E upon adsorption reaches 4%. The 1200°C annealing restores the initial Young's modulus while water vapour adsorption decreases it slightly. It is to be noticed that the relative mass gain at saturation is as low as 10^{-4} g/g instead of 3×10^{-3} g/g for chalk. This agrees with the fact that at 50% RH, the coverage of physisorbed water reaches a monolayer on most technical surfaces.

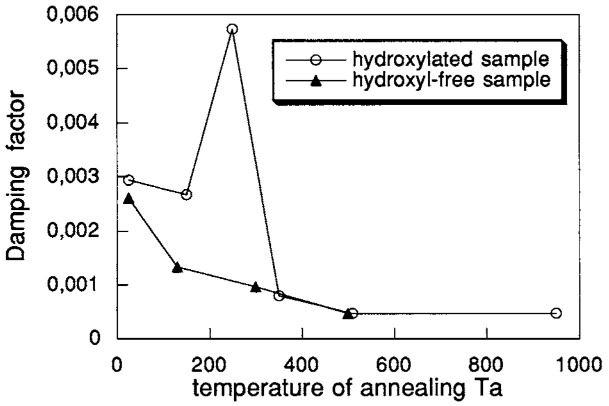

Figure 9 Damping factor of water-free alumina samples after annealing at various temperatures. On gibbsite-containing sample the behaviour at low temperature is dominated by the decomposition of gibbsite.

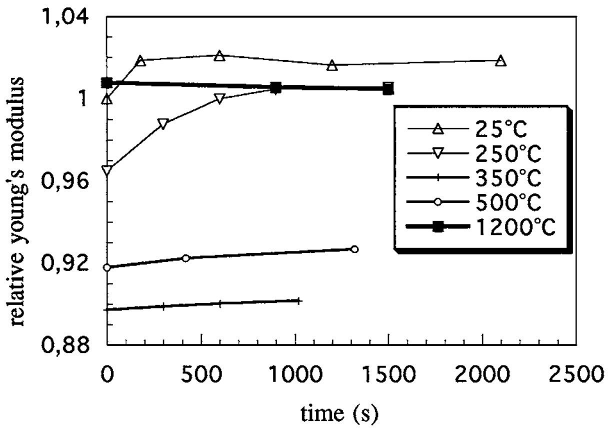

Figure 10 Young's modulus of a gibbsite containing sample during water adsorption from the laboratory air after annealing at selected temperatures.

2.2.2.2. *Drying of samples previously soaked in water*

Damping factor. As illustrated in Fig. 1, after saturation of the adsorption from the laboratory air, the sample is soaked in distillated water for 300 s, then the mechanical properies are measured during subsequent drying. In Fig. 11, $Q^{-1}_{(\mathrm{Sw})}$ is plotted for various annealing

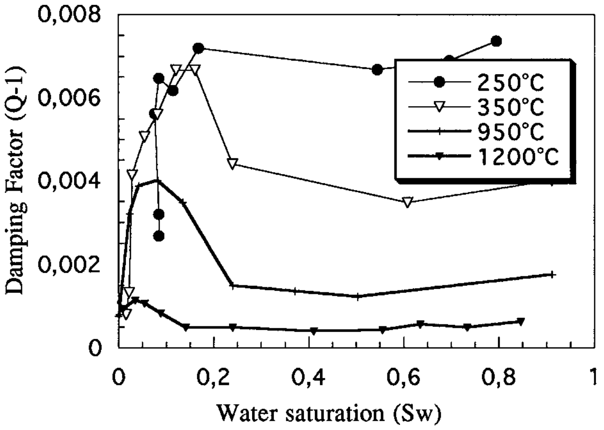

Figure 11 Damping factor of a gibbsite containing sample during drying. The maximum of the damping factor is apparent only at intermediate annealing temperatures.

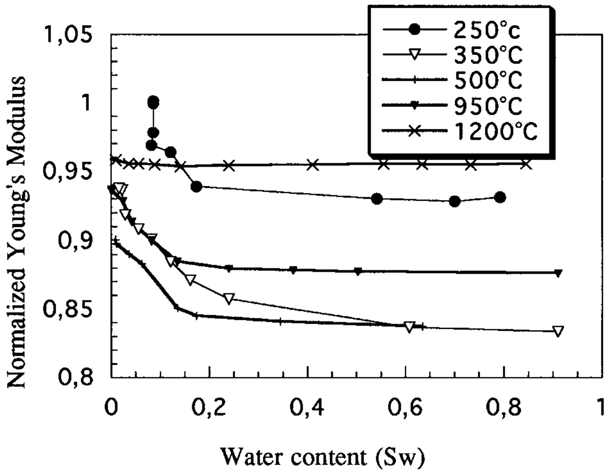

Figure 12 Young's modulus of a gibbsite containing sample during drying after annealing at various temperatures.

temperatures T_a up to 1200°C. At intermediate annealing temperatures, $Q^{-1}_{(\mathrm{Sw})}$ exhibits a large peak near the dry state. This peak cannot be resolved neither on the $T_a = 250$°C curve where the damping factor is high, nor on the $T_a = 1200$°C curve where Q^{-1} is very low.

Young's modulus. Fig. 12 represents the evolution of the Young's modulus as a function of the water content during drying after annealing at increasing temperatures. The sample is a hydroxylated one that suffers a 6×10^{-3}g/g mass loss on heating at 1200°C. The variation between the dry and the wet state is maximum on the 350°C heated sample and practically nil after annealing at 1200°C. This coroborates the damping factor evolution. The same variations, either against the temperature of annealing or the water content on a sample initially devoid of hydroxyls that suffers a mass loss lower than 1×10^{-4} g/g on heating at 1200°C, can be noticed (Fig. 13). However, due to the low hydroxyl content of the material, the variations are much more reduced. The results on Young's modulus are gathered in Fig. 14 where the open symbols refer to the dry state and the filled symbols to water soaked saturated samples. It is to be noticed that a small difference persists between the wet and the dry state, even after a 1200°C annealing.

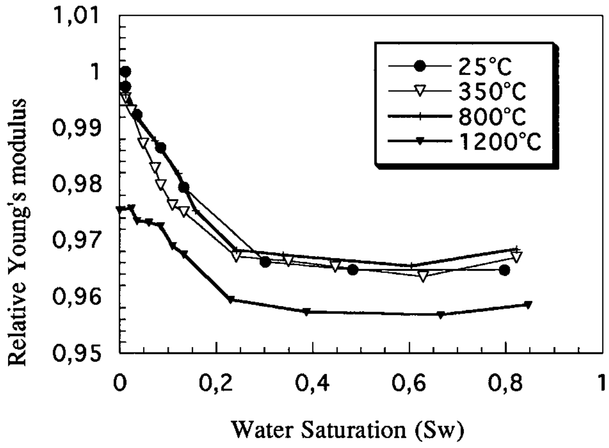

Figure 13 Young's modulus during drying of a gibbsite free sample after annealing at various temperatures.

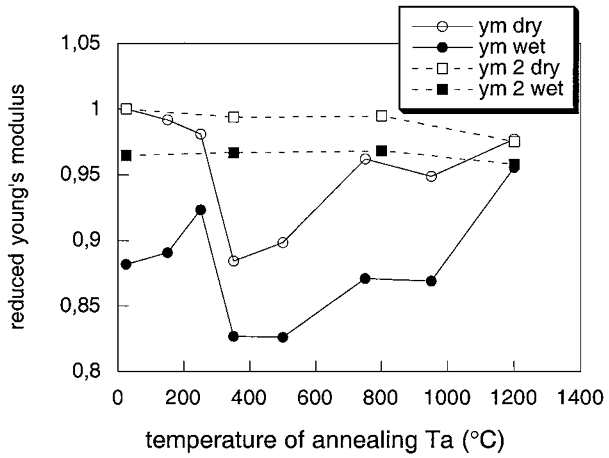

Figure 14 Variations of the Young's modulus as a function of the temperature of annealing T_a for a gibbsite-free sample (square symbols) and a gibbsite-containing sample (circles). Open symbols refer to the dry state, filled symbols to the water saturated state.

2.2.3. Rehydroxylated samples

It appears that the hydroxyl content of the sample governs its behaviour towards water. Up to now, only dehydroxylation experiments have been performed. Otherwise it is said that alumina undergoes rapid rehydroxylation when put in contact with water [16]. Fig. 15

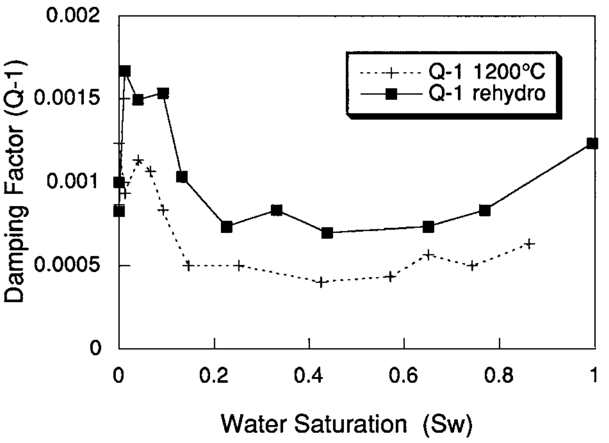

Figure 15 $Q^{-1}_{(\mathrm{Sw})}$ curves for a thoroughly dehydroxylated sample (Q^{-1} 1200°C) and after hydrothermal treatment leading to rehydroxylation (Q^{-1} rehydro).

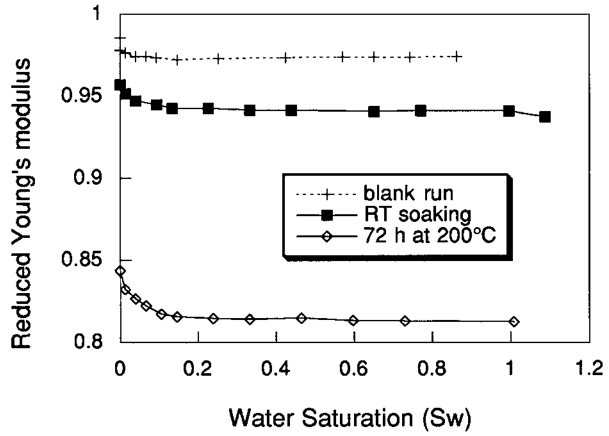

Figure 16 $E_{(\mathrm{Sw})}$ curves for a thoroughly dehydroxylated sample and after hydrothermal treatment leading to rehydroxylation.

and Fig. 16 represent the evolution of $Q^{-1}_{(\mathrm{Sw})}$ and $E_{(\mathrm{Sw})}$ after hydrothermal treatments that are claimed to lead to rehydroxylation of alumina. The Young's modulus is highly sensitive to the hydroxyl content. The hydrothermal treatment, 72 h at 200°C in liquid water under the corresponding vapour pressure, results in a 20% lowering of the Young's modulus although no mass gain can be measured on rehydroxylation at the detection limit of 5×10^{-5} g/g. The corresponding two fold increase in $Q^{-1}_{(\mathrm{Sw})}$ on rehydroxylation proves one more time that mechanical damping by water is linked to the hydroxyl content of the porous medium. The Young's modulus of a virgin, hydroxyl-containing sample, is 30% lower than that of a hydroxyl-free one (90 GPa instead of 120 GPa). This cannot be explained by changes in porosity [4, 5]. These experiments also prove that during a typical experiment (300 s soaking in water then drying), rehydroxylation can be neglected.

2.2.4. Silica and graphite

Results on porous silica glass (Vycor) and graphite, previously presented [2, 3] need to be revisited. On Vycor, results presented on Fig. 17 reproduced from Ref. 2 correspond to those presented on Fig. 8 for alumina and on Fig. 3 for chalk. Because of the large surface area of Vycor (200 m^2/g) adsorption from the laboratory air results in a large increase in mass and results are presented as a function of the water saturation Sw instead of time as in Fig. 8. Some results are relevant to the problem. On one hand, as dehydroxylation proceeds, the initial value (i.e. the water-free value) of the damping factor does not change. Furthermore the initial slope $\frac{dQ^{-1}_{(\mathrm{Sw})}}{d\mathrm{Sw}}$ is also insensitive to the hydroxyl content of the sample. On the other hand, the Sw and $Q^{-1}_{(\mathrm{Sw})}$ values at the knees of the curves are the smallest at high annealing temperature. These results agree with the following model.

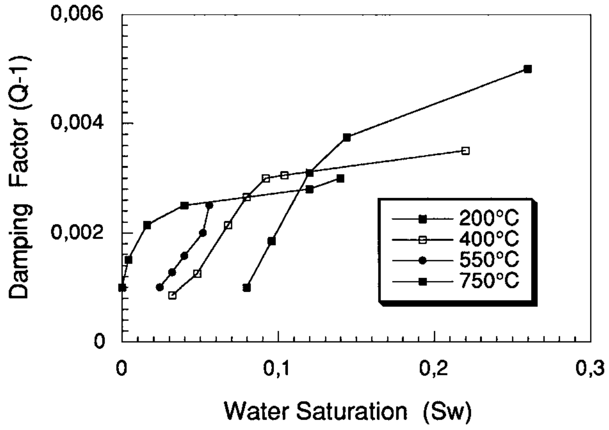

Figure 17 $Q^{-1}_{(\mathrm{Sw})}$ curves on Vycor during adsorption of water vapour from the laboratory air after annealing at various temperatures. This figure is to be compared with Fig. 8.

On silica, bound water is linked to surface hydroxyls. It is generally admitted that one water molecule is bound by H-bonding to two hydroxyls [7, 10]. These sole species (water molecules H-bonded to hydroxyls) are responsible for the damping of mechanical vibrations in the sonic range. Neither hydroxyls that are too firmly attached to the substrate, nor free water too loosely bound to the surface, are able to dissipate mechanical energy [17]. This contradicts early models where geminal silanols, H-bonded to each other, were supposed to dissipate energy [3, 11, 14]. According to this refined model, hydroxyls do not dissipate energy by themselves, but on most substrates, especially oxides, they act as binding sites for molecular bound water which is the truly dissipating species.

Infra-red spectroscopy is a valuable tool to distinguish bound water from free water. On Fig. 18, reproduced from Ref. 1, the absorbance peak at 5260 cm^{-1} corresponds to water H-bonded to the hydroxyls while the shoulder around 5200 cm^{-1} is attributed to free water in the liquid state [7]. On fully hydroxylated surfaces this shoulder appears at $\mathrm{Sw} = 0.16$, i.e. near the completion of the first H-bonded water layer (in a sample with $A_s = 200\ m^2/g$ a water monolayer corresponds to $\mathrm{Sw} = 0.24$). On silica partly dehydroxylated by heat treatment, this peak occurs at lower water coverage as shown on Fig. 18. The water content at the appearance of the 5200 cm^{-1} shoulder corresponds closely to the water content at the knees in the $Q^{-1}_{(\mathrm{Sw})}$ curves of Fig. 17.

Results presented on Fig. 3 of Ref. [2] show that on dehydroxylated silica surfaces, the Young's modulus is decreased by water adsorption as in the case of the 1200°C heated alumina while on hydroxylated or virgin surfaces, water vapour adsorption increases it. This is easily explained by changes in the state of adsorption of water. On hydroxylated surfaces, the network of H-bonded water molecules reinforces the stiffness of the sample. On hydroxyl-free surfaces no lateral interaction can take place between the neighbouring water molecules. On Fig. 19 the thermal desorption spectra of physisorbed water from a Vycor sample equilibrated at room temperature after a 250°C and after a 650°C anneal are shown. On the 250°C annealed, i.e. fully hydroxylated sample, the ratio of free water desorbable below 105°C to bound water desorbable in the range 105°C–250°C is 0.9. After a 650°C anneal, this ratio is larger than 4. According to Iler [10], a fully hydroxylated silica surface bears 4.6 OH nm^{-2} but after a 650°C anneal, the OH coverage is reduced to 1.3 OH nm^{-2}. This correlates well with the change

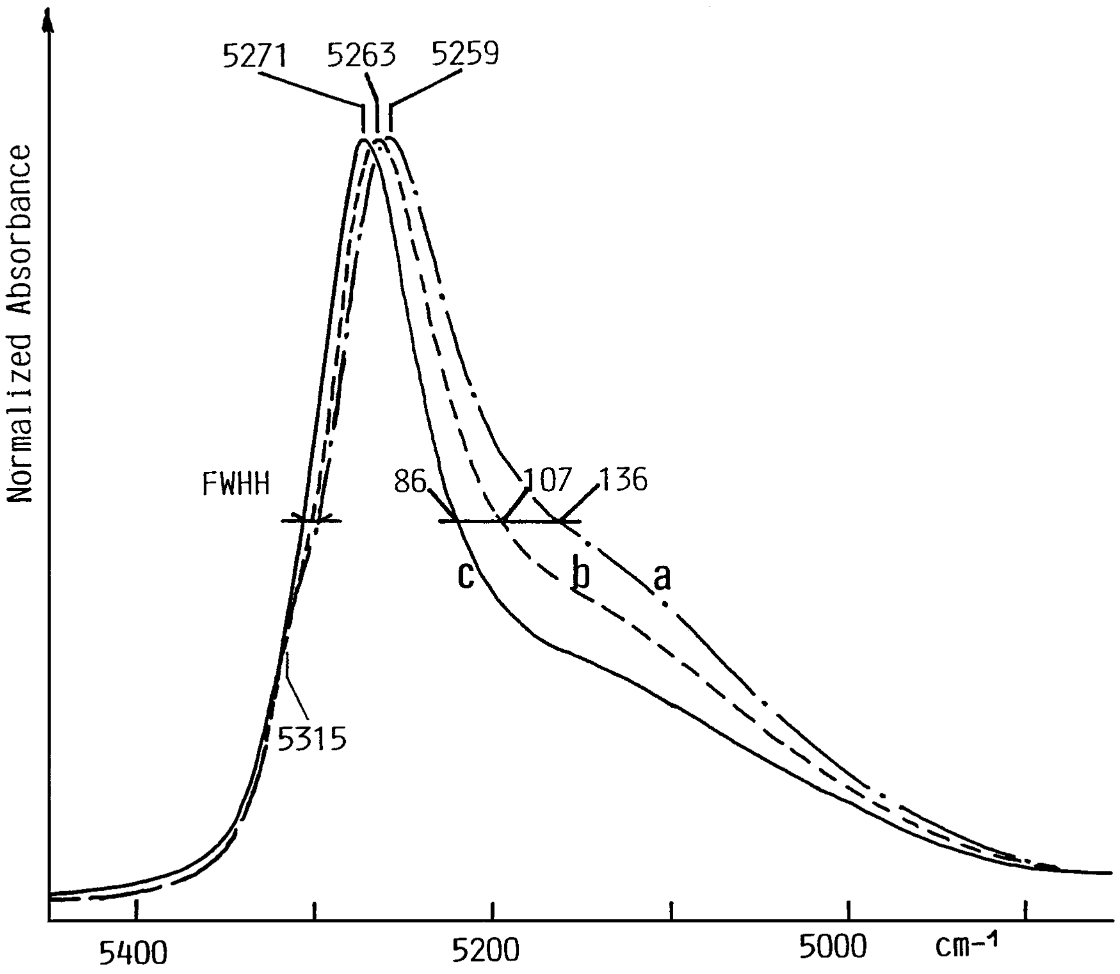

Figure 18 Comparison between absorbance profiles, normalized at maxima, of water absorbed on porous Vycor 7930 glass after annealing at three temperatures. The spectrum variations correspond to similar mass percentages of water for all temperatures: (a) after 130°C annealing: 1.4%–0.5% ; (b) after 450°C annealing: 1.4%–0.8%; (c) after a 650°C annealing: 1.3%–0.6%. FWHH gives the fullwidth at half height of the three bands.

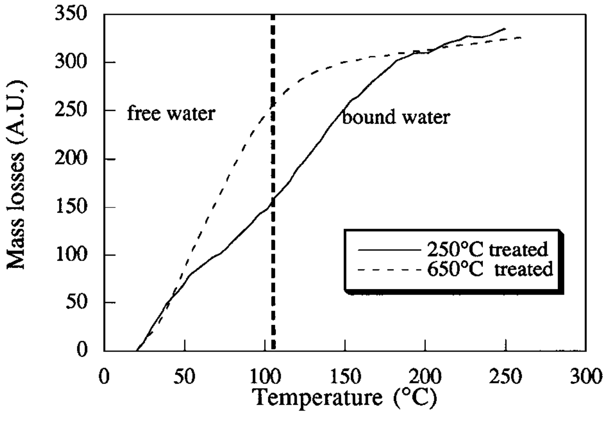

Figure 19 Thermogramm of a Vycor sample equilibrated at the laboratory air (RH = 50%) after two annealings. Temperatures of annealing: full line 250°C, dotted line 650°C.

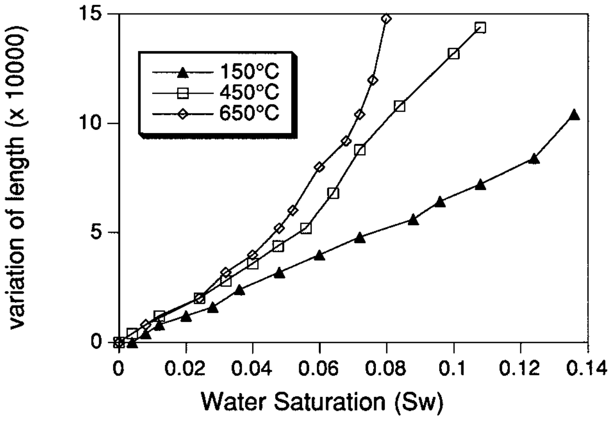

Figure 20 Relative length changes of a Vycor sample during adsorption of water vapour after heating at the indicated temperatures.

in bound water coverage upon annealing as revealed by thermal desorption and by our mechanical experiments. It appears that adsorption of water in the bound state stiffens the sample, a result that seems reasonable. More surprising is the weakening of the substrate by free water, since it is expected that only weak dispersive forces are operating in this case.

Perhaps the more illustrative results relate to swelling, i.e. changes of length as a function of the adsorption of water vapour. On Fig. 20, reproduced from Ref. [1], the room temperature change of length $\frac{\Delta L}{L}$ of a Vycor sample is plotted as a function of the water saturation Sw during adsorption for three temperatures of annealing T_a. The 150°C annealing curve is linear up to Sw = 0.13. On the 450°C and 650°C curves the upward inflexion can be resolved at a much lower water saturation. The water content at these points is identical to that at the knees on the curves in Fig. 17. Changes in length have been attributed to adsorbate-substrate in-

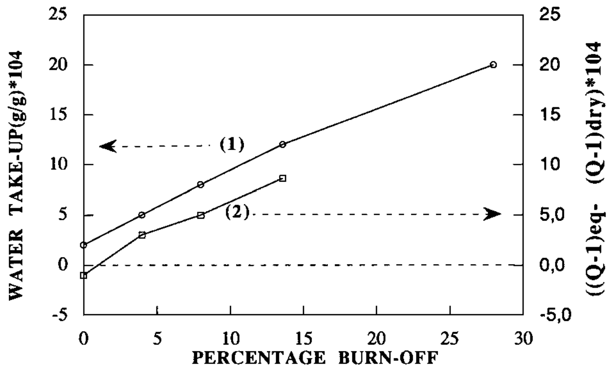

Figure 21 Amount of water vapour (1) measured by gravimetry in g/g, adsorbed on a porous graphite sample after the burning-off of graphite in air at 550°C and subsequent changes in the damping factor (2). On the right hand side of the figure the plotted parameter is $(Q^{-1})_{\text{eq}} - Q^{-1})_{\text{dry}}$ where $(Q^{-1})_{\text{eq}}$ refers to a sample equilibrated at the laboratory air and $Q^{-1})_{\text{dry}}$ refers to a sample in a dry state after heating at 150°C.

teractions [18–21]. Low dilatation or even contraction result from H-bonding interaction that attract the inner parts of the pores [19]. When only dispersive forces are operative, as in the case of rare gas adsorption at low temperature, the dilatation is largest [20]. Studies on swelling of porous media during adsorption corroborate measurement of elastic properties. H-bonding of the adsorbate to the substrate stiffens the composite while adsorption by dispersive forces weaken it. It is well known that hydroxyl-free oxide surfaces are hydrophobic and on these surfaces, adsorbate-absorbent interactions are reduced to van der Waals forces.

Similar conclusions can be drawn from results on graphite presented in Fig. 21, taken from Ref. [3]. As burn-off in air proceeds, graphite turns to be more and more hydrophilic as shown on the curve (1) of Fig. 21. At the same time, the damping factor of the air equilibrated sample increases over the water-free value (curve (2)). It is to be noticed that at zero burn-off, i.e. on oxygen-free samples, water adsorbs in the so-called free state up to 2×10^{-4} g/g and that in this case water vapour adsorption lowers the damping factor (the ordinate of the first point on curve (2) is negative). As burn-off proceeds more and more oxygen atoms are incorporated to the surface that provide polar sites for water adsorption [22, 23]. Water binds by H-bonding on these oxygenated sites leading to enhanced mechanical dissipation. In this case also, the damping factor at zero water coverage does not depend on the oxygen coverage as well as the damping of Vycor at $\text{Sw} = 0$ does not depend on the tightly bound species (hydroxyls) coverage. It is expected that strongly adsorbed oxygen species, designated as surface oxides, do not damp the host medium. However this conclusion must be mitigated since the oxygen coverage is not precisely known in these experiments.

This shed some light on the results presented in Fig. 8 where the damping factor of alumina at zero water coverage is plotted against the temperature of annealing. On gibbsite-free sample Q^{-1} decreases slowly till 500°C where obviously molecular water is absent. However most of the decrease occurs below 200°C i.e. during desorption of bound water. The results on gibbsite containing sample are of poor interest in this case because of the large structural changes that accompany gibbsite decomposition.

3. Discussion

In a previous publication [3], the dependence of the damping factor Q^{-1} on the content of hydrogenated species has been written as the sum of three terms.

$$Q^{-1} = Qo^{-1} + k_1[\text{OH}][\text{H}_2\text{O}] + k_2[\text{OH}_\alpha]^2 \qquad (2)$$

where Qo^{-1} is the intrinsic damping factor that depends largely on the structure of the material. In the third term $k_2[\text{OH}_\alpha]^2$ it is recognised that only weakly bound hydroxyls H-bonded to themselves participate to damping. These species are called OH_α in contradistinction to isolated, tightly bound hydroxyls. It seems more advisable to classify these species as tightly bound water molecules and the third term of Equation 2 can be discarded. In the second term $k_1[\text{OH}][\text{H}_2\text{O}]$, the hydroxyl concentration [OH] can be dropped out since the concentration of bound water $[(\text{H}_2\text{O})_\text{b}]$ is related to the to the hydroxyl content [OH]. It is generally accepted that a water molecule is linked to two hydroxyls and $[(\text{H}_2\text{O})_\text{b}] = \frac{1}{2}[\text{OH}]$. Finally, a more accurate and simple expression of (2) would be

$$Q^{-1} = Qo^{-1} + k[(\text{H}_2\text{O})_\text{b}]. \qquad (3)$$

that illustrates the prominent role of bound water.

During adsorption of water, Q^{-1} reflects the kinetics of adsorption of bound water that occurs at relative humidity as low as 10%. This explains for instance the results of numerous authors who found a rapid increase of the damping factor at RH as low as 10% [11, 14, 24–27]. At saturation Q^{-1} reflects the state of hydroxylation of the surface, a fact that has never been pointed out before.

4. Conclusion

In this experimental paper, evidences have been afforded for the H-bonding of water in porous media and its influence on mechanical damping. A clear distinction is made between bound and free water. On most materials, bound water is associated with polar sites (hydroxyls groups on oxides, surface oxides on graphite). On calcite where the surface chemistry is not so well documented, a pertinent parameter would be the temperature of desorption of water. Free water is bound to surfaces by weak van der Waals forces, its desorption temperature is below 105°C. Bound water desorption temperature lies in the 105°C–250°C range. In contradistinction with a widely spread opinion, free water is harmful to the cohesive properties of the solids. This is reflected in this study by the decrease of the Young's modulus and the enhanced swelling upon adsorption of water on non-polar surfaces. In the following paper, the experimental facts presented here are taken into account in order to discuss the nature of the maximum in the $Q^{-1}(\text{Sw})$ curve.

References

1. A. BURNEAU, J. LEPAGE and G. MAURICE, *J. Non-Cryst. Solids* **217** (1997) 1.
2. J. LEPAGE, A. BURNEAU, N. GUYOT and G. MAURICE, *ibid.* **217** (1997) 11.
3. J. LEPAGE and J. MENAUCOURT, *J. Mat. Sci.* **33** (1998) 2905.
4. "CRC Handbook of Chemistry and Physics," 78th ed, p. 12–38 and 12–40.
5. R. W. RICE, *J. Mat. Sci.* **31** (1996) 1509.
6. K. R. LANGE, *J. Colloid Sci.* **20** (1965) 231.
7. A. BURNEAU, O. BARRÈS, J. P. GALLAS and J. C. LAVALLEY, *Langmuir* **6** (1990) 1364.
8. G. WIRZING, *Naturwissenschaften* **50** (1963)
9. G. J. YOUNG, *J. Colloid Sci.* **13** (1958) 67.
10. R. K. ILER, "The Chemistry of Silica" (John Wiley, New York, (1979) chap. 6.
11. W. F. MURPHY, III, *J. Acoust. Soc. Am.* **71** (1982) 1458.
12. T. BOURBIÉ and B. ZINSZNER, *J. Geophys. Res.* **90** (1985) 11524.
13. E. J. SCHMIDT, D. VO-THANH, A. NUR and B. AULD, Stanford University Research Paper, unpublished.
14. V. A. CLARK, B. R. TITTMANN and T. W. SPENCER, *J. Geophys. Res.* **85** (1980) 5190.
15. M. RODAHL, F. HÖÖK, C. FREDRIKSSON, C. A. KELLER, A. KROZER, P. BRZEZINSKI, M. VOINOVA and B. KASEMO, *Faraday Discuss.* **107** (1997) 229.
16. S. G. GREGG and K. S. W. SING, in "Adsorption, Surface Area and Porosity" (Academic Press, London, 1982) p. 274.
17. E. FORSLIND and A. JACOBSSON, in "Water. A Comprehensive Treatise," Vol. 5, edited by F. Franks (Plenum Press, New York, 1975) p. 274.
18. Y. KOZIROVSKI and M. FOLMAN, *Trans. Farad. Soc.* **58** (1962) 2228.
19. M. FOLMAN and D. J. C. YATES, *ibid.* **54** (1958) 429.
20. *Idem., ibid.* **54** (1958) 1624.
21. D. J. C. YATES, *Proc. Roy. Soc. London* **A 224** (1954) 526.
22. P. L. WALKER and J. JANOV, *J. Colloid Interface Sci.* **28** (1968) 107.
23. B. BRAND and R. ROBINSON, *Carbons* **15** (1968) 257.
24. B. I. PANDIT and M. S. KING, *Can. J. Earth Sci.* **16** (1979) 2187.
25. B. R. TITTMANN, in Proc. IEEE Ultrasonics Symposium (Institute of the Electrical and Electronics Engineers, New York, 1979) p. 327.
26. V.A. CLARK, T. W. SPENCER and B. R. TITTMANN, *J. Geophys. Res.* **86** (1981) 7087.
27. B .R. TITTMANN, V. A. CLARK, J. M. RICHARDSON and T. W. SPENCER, *ibid.* **85** (1980) 5199.

Received 15 February 2000
and accepted 21 February 2001